

# Photoeffects in Thin-Film Molecular-Level Chromophore-Quencher Assemblies. 1. Physical Characterization

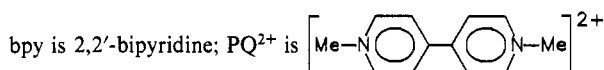
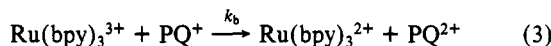
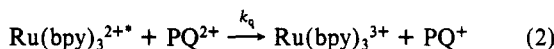
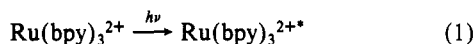
Nigel A. Surridge, Stephen F. McClanahan, Joseph T. Hupp, Earl Danielson, Sharon Gould, and Thomas J. Meyer\*

Department of Chemistry, The University of North Carolina, Chapel Hill, North Carolina 27599-3290  
(Received: June 1, 1987; In Final Form: June 17, 1988)

Molecular-level chromophore-quencher assemblies have been prepared in precast chlorosulfonated polystyrene ( $[-CH_2CH(p-C_6H_4SO_2Cl)]_x-$ ; PS- $SO_2Cl$ ) films by (1) exposing the intact film to solutions containing the chromophore  $[(bpy)_3Ru(5-NH_2phen)][PF_6]_2$  ( $bpy$  is 2,2'-bipyridine; 5- $NH_2phen$  is 5-amino-1,10-phenanthroline) which becomes chemically bound through sulfonamide bond formation, (2) partially hydrolyzing a portion of the remaining  $-SO_2Cl$  sites to  $-SO_3^-$  sites and exposing the resulting films to acetonitrile solutions containing the electron-transfer quencher paraquat ( $PQ^{2+}$ ) and the reductive scavenger triethanolamine ( $N(C_2H_4OH)_3$ ). The photophysical properties of the chromophore-based metal-to-ligand charge-transfer excited state have been investigated by lifetime and visible absorption and emission spectra. Although similar to related monomers, excited-state decay in the films is nonexponential. The dynamics of excited-state quenching by  $PQ^{2+}$  following pulsed laser excitation show that the chromophore occupies three different chemical sites within the films. At one site, which accounts for  $\sim 50\%$  of the emitted light and appears to be located near ion channels created by hydrolysis, quenching is rapid,  $K_{SV} \sim 6.8 \times 10^4 M^{-1}$ . A second site exists that undergoes relatively slow quenching,  $K_{SV} \sim 3 \times 10^3 M^{-1}$ , and then only with added  $[NEt_4](ClO_4)$ . A third site is present that is not quenched.

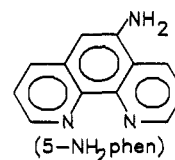
## Introduction

Metal-to-ligand charge-transfer (MLCT) excited states of polypyridyl complexes of Ru(II), Os(II), or Re(I) characteristically undergo rapid oxidative or reductive electron-transfer quenching in solution to give reasonable yields of separated redox products, for example, reactions 1 and 2.<sup>1</sup> Although large amounts of



transiently stored redox energy can be produced in solution-based systems with relatively high yields, the subsequent capture of the stored redox equivalents is severely limited by back electron transfer, e.g., reaction 3. A number of attempts to control the excitation/quenching/electron transfer sequence have been reported based on intramolecular systems including chromophore-quencher complexes and ligand-bridged complexes,<sup>2</sup> soluble polymers,<sup>3</sup> vesicles,<sup>4</sup> and polymeric films on electrodes.<sup>5,6</sup>

We have described the design of a series of photoelectrodes<sup>7</sup> based on oxidative quenching by  $PQ^{2+}$ , of the MLCT excited states of  $Ru(5-NH_2phen)_3^{2+}$  (5- $NH_2phen$  is 5-amino-1,10-phenanthroline) and related complexes covalently bound via



sulfonamide links within polymeric films of chlorosulfonated polystyrene.<sup>8</sup> Our choice of chlorosulfonated polystyrene was deliberate in that the underlying synthetic chemistry appeared to offer a basis for the preparation of controlled microstructures within the polymeric film environment. The thought was that in an appropriately designed microstructure it might be possible to deliver the photochemically produced oxidizing and reducing equivalents to different parts of the film, thus providing a molecular analog of the p/n junction in a semiconductor solar cell.<sup>9</sup>

With such a goal in mind, film-based systems that utilize a chemically reactive polymer like chlorosulfonated polystyrene (PS- $SO_2Cl$ ) offer some important advantages. The chromophore-quencher apparatus can be assembled in fixed sites after the film has been cast, based on the formation of chemically stable

(1) (a) Sutin, N.; Creutz, C. *Pure Appl. Chem.* **1980**, *52*, 2717. (b) Sutin, N. *J. Photochem.* **1979**, *10*, 19. (c) Balzani, V.; Bolletta, F.; Gandolfi, M. T.; Maestri, M. *Top. Curr. Chem.* **1978**, *75*, 1. (d) Kalyanasundaram, K. *Coord. Chem. Rev.* **1982**, *46*, 159. (e) Meyer, T. J. *Acc. Chem. Res.* **1978**, *11*, 94. (f) Meyer, T. J. *Prog. Inorg. Chem.* **1983**, *30*, 389. (g) Balzani, V.; Scandola, F. In *Energy Resources through Photochemistry and Catalysis*; Gratzel, M., Ed.; Academic: New York, 1983; Chapter 1.

(2) (a) Liddell, P. A.; Barrett, D.; Makings, L. R.; Pessiki, P. J.; Gust, D.; Moore, T. A. *J. Am. Chem. Soc.* **1986**, *108*, 5350. (b) Kanda, Y.; Sato, H.; Okada, T.; Mataga, N. *Chem. Phys. Lett.* **1986**, *129*, 306. (c) Warman, J. M.; DeHass, P.; Oevering, H.; Verhoven, J. W.; Paddon-Row, M. N.; Oliver, A. M.; Hush, N. S. *Chem. Phys. Lett.* **1986**, *128*, 95. (d) Danielson, E.; Elliott, C. M.; Merkert, J. W.; Meyer, T. J. *J. Am. Chem. Soc.* **1987**, *109*, 2519. (e) Schanze, K. S.; Neyhart, G. A.; Meyer, T. J. *J. Phys. Chem.* **1986**, *90*, 2182. (f) Meyer, T. J. *NATO ASI, Ser. C* **1987**, *214*, 103.

(3) (a) Sasson, R. E.; Gershuni, S.; Rabani, J. *J. Phys. Chem.* **1985**, *89*, 1937. (b) Sumi, K.; Furue, M.; Nozakura, S.-I. *J. Polym. Sci., Polym. Chem. Ed.* **1984**, *22*, 3779. (c) Hirabaru, O.; Nakase, T.; Hanabusa, K.; Shivali, H.; Takemoto, K.; Hojo, N. *J. Chem. Soc., Dalton Trans.* **1984**, 1485. (d) Hargreaves, J. S.; Webber, S. E. *Macromolecules* **1984**, *17*, 235. (e) Margerum, L. D.; Murray, R. W.; Meyer, T. J. *J. Phys. Chem.* **1986**, *90*, 728. (f) Sasson, R. E.; Rabani, J. *J. Phys. Chem.* **1985**, *89*, 5500. (g) Margerum, L. D.; Murray, R. W.; Meyer, T. J. *J. Phys. Chem.* **1986**, *90*, 2696. (h) Olmsted III, J.; McClanahan, S. F.; Danielson, E.; Younathan, J. N.; Meyer, T. J. *J. Am. Chem. Soc.* **1987**, *109*, 3297.

(4) (a) Arrhenius, T. S.; Blanchard-Desce, M.; Dvornitzky, M.; Lehn, J.-M.; Malthete, J. *Proc. Natl. Acad. Sci. U.S.A.* **1986**, *83*, 5355. (b) Mettee, H. D.; Ford, W. E.; Sakai, T.; Calvin, M. *Photochem. Photobiol.* **1984**, *39*, 679. (c) Wohlgenuth, R.; Orvos, J. W.; Calvin, M. *Proc. Natl. Acad. Sci. U.S.A.* **1982**, *79*, 5111. (d) Fendler, J. H. *J. Phys. Chem.* **1985**, *89*, 2730.

(5) (a) Westmoreland, T. D.; Calvert, J. M.; Murray, R. W.; Meyer, T. J. *J. Chem. Soc., Chem. Commun.* **1983**, 65. (b) Margerum, L. D.; Meyer, T. J.; Murray, R. W. *J. Electroanal. Chem.* **1983**, *149*, 279.

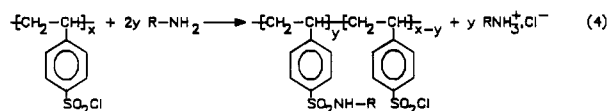
(6) (a) Kaneko, M.; Yamada, A. *Electrochim. Acta* **1986**, *31*, 273. (b) Oyama, N.; Yamaguchi, S.; Kaneko, M.; Yamada, A. *J. Electroanal. Chem.* **1982**, *139*, 215. (c) Morishima, Y.; Fukushima, Y.; Nozakura, S. *J. Chem. Soc., Chem. Commun.* **1985**, 912. (d) Yamamura, T.; Umezawa, Y. *J. Chem. Soc., Dalton Trans.* **1982**, 1977. (e) Kaneko, M.; Moriya, S.; Yamada, A.; Yamamoto, H.; Oyama, N. *Electrochim. Acta*, **1984**, *29*, 115. (f) Kaneko, M.; Yamada, A.; Oyama, N. *Nippon Kagaku Kaishi* **1984**, *11*, 1810. (g) Majda, M.; Faulkner, L. R. *J. Electroanal. Chem.* **1984**, *169*, 77; **1984**, *169*, 97.

(7) (a) Hupp, J. T.; Otruba, J. P.; Parus, S. J.; Meyer, T. J. *J. Electroanal. Chem.* **1985**, *190*, 287. (b) Hupp, J. T.; Meyer, T. J. *J. Electroanal. Chem.* **1987**, *224*, 59. (c) Hupp, J. T.; Meyer, T. J., submitted for publication.

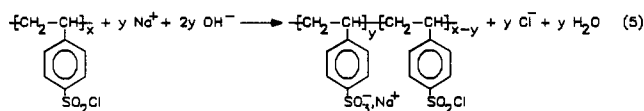
(8) Ellis, C. D.; Meyer, T. J. *Inorg. Chem.* **1984**, *23*, 1748.

(9) Fahrenbruch, A. L.; Bube, R. H. *Fundamentals of Solar Cells*; Academic: New York, 1983.

sulfonamide links (eq 4) or by partial hydrolysis, which provides



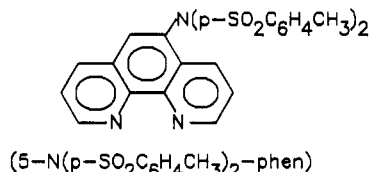
a basis for the incorporation of mobile cationic electron transfer carriers (eq 5).



We describe here in considerable detail the preparation and physical characterization of a film-based chromophore-quencher system that utilizes a chemically bound, fixed-site Ru-bpy chromophore and  $\text{PQ}^{2+}$  as a mobile quencher.

### Experimental Section

**Materials.** The salt  $[\text{Ru}(\text{bpy})_2(5\text{-NH}_2\text{phen})](\text{PF}_6)_2$  was prepared and purified as previously described.<sup>10</sup> The preparation of the model complex  $[(\text{bpy})_2\text{Ru}(5\text{-N}(p\text{-SO}_2\text{C}_6\text{H}_4\text{CH}_3)_2\text{phen})](\text{PF}_6)_2$  by the reaction between  $[(\text{bpy})_2\text{Ru}(5\text{-NH}_2\text{phen})]^{2+}$  and  $p\text{-ClSO}_2\text{C}_6\text{H}_4\text{CH}_3$  has also been described.<sup>11</sup>



$[\text{Zn}(5\text{-NH}_2\text{phen})_3](\text{PF}_6)_2$  was prepared by dissolving 200 mg (1.02 mmol) of 5-amino-1,10-phenanthroline in 15 mL of boiling absolute ethanol and adding 76 mg (0.34 mmol) of zinc acetate dissolved in 5 mL of water. The precipitate, which formed immediately, was collected and dissolved in water. The addition of an aqueous solution of  $\text{NH}_4\text{PF}_6$  precipitated the yellow complex, which was recrystallized from  $\text{CH}_3\text{CN}$  and water. Chlorosulfonated polystyrene,  $\text{PS-SO}_2\text{Cl}$ , was prepared by treatment of polystyrene ( $M_w = 4000$ ,  $M_w/M_n = 1.04$ , Polyscience, Inc.) with  $\text{HSO}_3\text{Cl}$  in  $\text{CCl}_4$  at  $0^\circ\text{C}$  and characterized for chloride content as described in the literature.<sup>8,12</sup> Tetraethylammonium perchlorate (TEAP) was used as received from G. F. Smith Chemical Co. The  $\text{PF}_6^-$  salt of  $\text{PQ}^{2+}$ ,  $\text{PQ}(\text{PF}_6)_2$ , was prepared from the  $\text{Br}^-$  salt and recrystallized two times from methanol/water. The remaining oxidative quenchers listed in Table II were prepared as described previously.<sup>13</sup> Reagent grade triethanolamine (TEOA) (G. F. Smith Chemical Co.) and 2-butanone (Aldrich) were used as received or distilled first with equivalent results. Acetonitrile (Burdick and Jackson) was stored over 4-Å molecular sieves.

**Preparation of Polymeric Films.** Typically, a 10- $\mu\text{L}$  aliquot of an acetone solution containing  $\text{PS-SO}_2\text{Cl}$  (0.4–1.0 mg/mL) was syringed onto a 0.125-cm<sup>2</sup> Teflon-shrouded Pt disk electrode (polished on a Buehler polishing wheel by using 5- $\mu\text{m}$  alumina or 1- $\mu\text{m}$  diamond paste) under inert atmosphere conditions. Following evaporation of the solvent, the resulting polystyrene film was allowed to dry under vacuum for at least 1 h (preferably overnight). For the preparation of films on larger surface areas, the volume of polymer solution used was adjusted such that a

constant ratio of 80  $\mu\text{L}/\text{cm}^2$  was obtained. Preparation of films used for FTIR, step profilometry studies, and photoelectrochemical studies, where it was desirable to maximize surface smoothness, involved spin casting the polymer onto flat glass/titanium/platinum substrates ( $1.14 \times 1.14 \times 0.04$  cm). A detailed account of the preparation of the electrodes appears in the following paper.<sup>14</sup> Films cast on these flat, platinum-covered glass slides facilitated IR analysis by using reflectance techniques. The casting procedure involved dropping  $\sim 0.01$  mL of a 0.2 M 2-butanone solution of the chlorosulfonated polystyrene onto a substrate slide spinning at 2000 rpm. This step was carried out with a Headway Research spin coater in an inert-atmosphere box, and the films were also vacuum dried prior to use. The use of smaller volumes of more concentrated  $\text{PS-SO}_2\text{Cl}$  solutions resulted in films with poor adhesive properties. Because of the limited solubility of  $\text{PS-SO}_2\text{Cl}$  in acetonitrile, the complex  $[\text{Ru}(\text{bpy})_2(5\text{-NH}_2\text{phen})]^{2+}$  was incorporated into the films simply by placing the precast film into an acetonitrile solution 5 mM in the complex at room temperature for a specified period of time and then rinsing the film well with fresh acetonitrile.

For experiments in which the films were subjected to hydrolysis, the film with or without chemically bound complex was placed in aqueous carbonate buffer (pH  $\sim 10$ , 0.5 M  $\text{Na}_2\text{CO}_3/0.5$  M  $\text{NaHCO}_3$ ) for periods of 1–3.5 h to hydrolyze some of the remaining sulfonyl chloride sites and thus impart an ion-exchange character. After hydrolysis, the films were rinsed with and soaked in distilled water for at least 20 min prior to rinsing with acetonitrile before being used.

**Measurements.** Cyclic voltammograms were recorded in a two-compartment cell with a PAR Model 175 universal programmer, a PAR Model 173 potentiostat, and a Hewlett-Packard Model 7015B X-Y recorder.

Electronic absorption spectra were recorded on Bausch and Lomb Spectronic 2000 or Hewlett-Packard 8450A diode array spectrophotometers. Emission spectra were obtained with an SLM Instruments, Inc., Series 8000 spectrofluorimeter using photon-counting techniques. Emission decay versus time curves were obtained with a PRA tunable dye laser by using coumarin 460-nm dye pumped by a PRA LN1000 pulsed  $\text{N}_2$  laser with a repetition rate of  $\sim 10$  Hz. The emission from films supported on a platinum slide in a Pyrex cell was detected by an EMI-Glencom, Inc., Model RFI/S PMT that was powered by a Fluke Model 412B high-voltage power supply. The slide was held in a solvent filled cell under Ar purge at  $45^\circ$  to both the excitation beam and to the entry slits of an ISA Instruments high-intensity monochromator. Decay signals were digitized by a LeCroy 9400 digital oscilloscope under the control of an IBM-PC, on which the data were stored and processed.

Infrared spectra of the spun-cast films were obtained with a Nicolet 20DX FTIR spectrometer and a Foxboro Model 9 multiple internal reflectance accessory equipped with a 20-cm KRS-5 crystal. The glass/titanium/platinum substrates with cast films were clamped against the front face of the KRS-5 crystal (similar spectra could be obtained with a Barnes Analytical 500 specular reflectance accessory).

Film thickness and smoothness measurements were carried out with a Tencor Alpha-Step 100 surface profilometer, while scanning electron microscopy was performed with an ISI-DS130 instrument.

### Results

**Film Characterization. Morphological Properties.** In Figure 1A is shown a scanning electron micrograph of a typical spun-cast  $\text{PS-SO}_2\text{Cl}$  polymeric film after sputter coating with  $\sim 50$  Å of gold to minimize charging effects. The film had been soaked in an acetonitrile solution containing  $[\text{Ru}(\text{bpy})_2(5\text{-NH}_2\text{phen})]^{2+}$  (5 mM) for 2 min and rinsed well with acetonitrile. The polymer in the upper section of the micrograph lies over a platinum covered area of the substrate to which it has adhered, whereas the bottom section is bare uncoated glass from which the polymer has peeled.

(10) Ellis, C. D.; Margerum, L. D.; Murray, R. W.; Meyer, T. J. *Inorg. Chem.* **1983**, *22*, 1283.

(11) Margerum, L. D. Ph.D. Dissertation, University of North Carolina at Chapel Hill, NC, 1985.

(12) (a) Rebek, J.; Gavina, F. J. *Am. Chem. Soc.* **1975**, *97*, 3453. (b) Siadat, B.; Lenz, R. W. J. *Polym. Sci., Polym. Chem. Ed.* **1980**, *18*, 3273.

(13) (a) Gutierrez, A. R. Ph.D. Dissertation, University of North Carolina at Chapel Hill, 1975. (b) Steckham, E.; Kuwana, T. *Ber. Bunsen-Ges. Phys. Chem.* **1974**, *78*, 253. (c) Homer, R. F.; Tomlinson, T. E. *J. Chem. Soc.* **1960**, 2498.

(14) Surridge, N. A.; Hupp, J. T.; McClanahan, S. F.; Meyer, T. J. *J. Phys. Chem.*, following paper in this issue.



TABLE I: Spectral and Photophysical Properties at 25 °C<sup>a</sup>

complex	MLCT			
	abs max		emission	
	$\lambda_{\max}$ , nm	fwhm, nm <sup>b</sup>	$\lambda_{\max}$ , nm	$\tau$ , ns
[(bpy) <sub>2</sub> Ru(5-NH <sub>2</sub> phen)] <sup>2+</sup>	456	~45	625	1150
[(bpy) <sub>2</sub> Ru(5-N( <i>p</i> -SO <sub>2</sub> C <sub>6</sub> H <sub>4</sub> CH <sub>3</sub> ) <sub>2</sub> phen)] <sup>2+</sup>	450	~45		1800 <sup>c</sup>
[(bpy) <sub>2</sub> Ru(5-(NHSO <sub>2</sub> -PS)phen)] <sup>2+</sup>	450	~67	616	$\tau_1 = 700^d$
film				$\tau_2 = 115^d$
[(bpy) <sub>2</sub> Ru(5-(NHSO <sub>2</sub> -PS)phen)] <sup>2+</sup>	452	~67	616	$\tau_1 = 578^d$
dissolved in DMSO				$\tau_2 = 124^d$

<sup>a</sup>In CH<sub>3</sub>CN for the soluble complexes. As films exposed to CH<sub>3</sub>CN solution for the polymers.  $\lambda_{\max}$  is for the most intense component in the visible spectra. <sup>b</sup>fwhm = full width at half-maximum for the band at the  $\lambda_{\max}$  cited. <sup>c</sup>In 1:1 CH<sub>3</sub>CN:H<sub>2</sub>O, ref 11. <sup>d</sup>Obtained by fitting the emission-time decay profiles to eq 8.

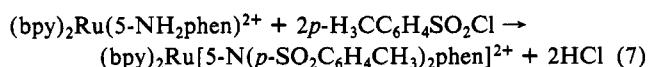
transition involving the primary amine group of the phenanthroline ligand. Protonation of the amine results in the disappearance of the transition as expected, and the band is absent in the model complex,<sup>11</sup> [(bpy)<sub>2</sub>Ru[5-N(*p*-SO<sub>2</sub>C<sub>6</sub>H<sub>4</sub>CH<sub>3</sub>)<sub>2</sub>phen)]<sup>2+</sup>. Electronic spectra taken on thin films immediately after soaking in a solution containing [Ru(bpy)<sub>2</sub>(5-NH<sub>2</sub>phen)]<sup>2+</sup> have an absorption band at 360 nm arising from the entrapped complex, which after it is removed, leaves the MLCT band for the sulfonamide bound complex at 455 nm. Under the same conditions the model complex [(bpy)<sub>2</sub>Ru(phen)]<sup>2+</sup> is also entrapped but can be completely removed by soaking in 0.1 M TEAP.

Absorption and emission spectra for the polymer-bound Ru complex both in the film and when the film is dissolved in dimethyl sulfoxide (DMSO) are compared to those of the related monomers in Table I (and Figure 2). The MLCT absorption band manifolds include contributions from  $d\pi \rightarrow \pi^*$  transitions to  $\pi^*$  levels on both the bpy and substituted phen ligands. MLCT band energies and shapes are sensitive to the surrounding environment and the broadening in the polymeric environment may, in part, be due to a matrix effect.

It is clear that only a small fraction of available -SO<sub>2</sub>Cl sites within the films are actually involved in chemical binding. For example, a film (3.2 × 10<sup>-5</sup> g/cm<sup>2</sup>) was cast onto a relatively large surface-area glass slide (4.5 cm<sup>2</sup>) and soaked in a 5 mM solution of [(bpy)<sub>2</sub>Ru(5-NH<sub>2</sub>phen)]<sup>2+</sup> for 2 h. After being rinsed with CH<sub>3</sub>CN and soaked in 0.1 M TEAP, the film was dissolved in 1.0 mL of DMSO, and an absorbance of 0.10 at 460 nm was measured. Assuming that  $\epsilon_{460} = 14\,500 \text{ M}^{-1} \text{ cm}^{-1}$  for the bound complex as for the monomer, it can be estimated that ~1% of the total -SO<sub>2</sub>Cl sites are chemically linked to the complex. However, for these soaking conditions in such relatively thick films, the complex appears to be confined to the outer portions of the film.<sup>15</sup> For complete loading in thin films, it has been estimated that up to ~49% of the total sites can be occupied by the rather large ( $r = 7 \text{ \AA}$ ) complex.<sup>8</sup>

We have attempted to obtain direct evidence for the sulfonamide link in the films by specular and multiple internal reflectance IR spectroscopy. However, due to the small effective path length and the relatively low loadings of metal complex (1–10%), only absorption features associated with the polymeric backbone were observable.

Attempts to form the metal-incorporated polymer in solution by dissolving both PS-SO<sub>2</sub>Cl and [(bpy)<sub>2</sub>Ru(5-NH<sub>2</sub>phen)]<sup>2+</sup> complex in DMF or acetone were unsuccessful. Only ion formation/association between the partially hydrolyzed poly-sulfonated polymer polyelectrolyte and metal complex was observed even when considerable effort was taken to exclude water from the reaction mixture. A sulfonamide containing monomeric complex was prepared by the reaction between *p*-toluenesulfonyl chloride and [Ru(bpy)<sub>2</sub>(5-NH<sub>2</sub>phen)]<sup>2+</sup> (eq 7) as described by



Margerum.<sup>11</sup> The relative rates of formation of the first and

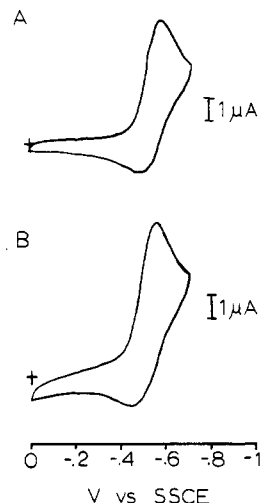


Figure 3. Cyclic voltammogram of the PQ<sup>2+/+</sup> couple with [PQ<sup>2+</sup>] ~ 0.25 mM in the external 0.1 M TEAP-CH<sub>3</sub>CN solution at 0.125 cm<sup>2</sup> electrodes coated with PS-SO<sub>2</sub>Cl films soaked in a 5 mM solution of [(bpy)<sub>2</sub>Ru(5-NH<sub>2</sub>phen)][PF<sub>6</sub>]<sub>2</sub> for 2 h (A) unhydrolyzed and (B) hydrolyzed for 3 h. Scan rate = 50 mV/s vs SSCE reference.

second sulfonamide bonds in solution are such that only the disubstituted complex could be prepared.

Cyclic voltammetric studies show the existence of a Ru(III/II) wave at +1.32 V vs SSCE in the films. However, a point that will play an important role later is that the Ru(III/II) wave can be observed only in thin films that have been exposed to the complex for extended periods of at least 2 h.

**Hydrolysis.** For experiments involving the generation of photocurrents<sup>7,14</sup> or for luminescence measurements, the films were hydrolyzed in aqueous carbonate buffers for periods of between 1 and 3.5 h following the incorporation of the metal complex. The efficiency of photocurrent production is highly dependent upon the degree of hydrolysis of the -SO<sub>2</sub>Cl sites to -SO<sub>3</sub><sup>-</sup> within the polymeric films. This was more or less an expected result since the mobility and extent of incorporation of the cationic quencher used, PQ<sup>2+</sup>, is expected to be significantly affected by the degree and location of hydrolysis within the film structure; the dynamics of quenching and redox product separation following photolysis could also be affected.

In a macroscopic sense, the hydrolysis step has a relatively small effect on the transport of PQ<sup>2+</sup> through the film to the inner electrode. The point is demonstrated by the cyclic voltammograms in Figure 3. From the data the cyclic voltammograms for the PQ<sup>2+/+</sup> couple with [PQ<sup>2+</sup>] ~ 0.25 mM in the external acetonitrile solution (Figure 3B) are only slightly affected by hydrolysis, suggesting that the bulk transport rate of the PQ<sup>2+/+</sup> couple through the film is only slightly affected as well.

The importance of the incorporation of PQ<sup>2+</sup> by ion exchange on the appearance of photocurrents was confirmed by a simple experiment. A film prepared on a platinum flag soaked for 2 h in 5 mM [(bpy)<sub>2</sub>Ru(5-NH<sub>2</sub>phen)][PF<sub>6</sub>]<sub>2</sub> was placed in a 0.1 M TEAP/acetonitrile solution where luminescence from the MLCT excited state was easily observed upon "black-light" irradiation.

(15) Surridge, N. A.; Linton, R. W.; Hupp, J. T.; Bryan, S. R.; Meyer, T. J.; Griggs, D. P. *Anal. Chem.* **1986**, *58*, 2443.

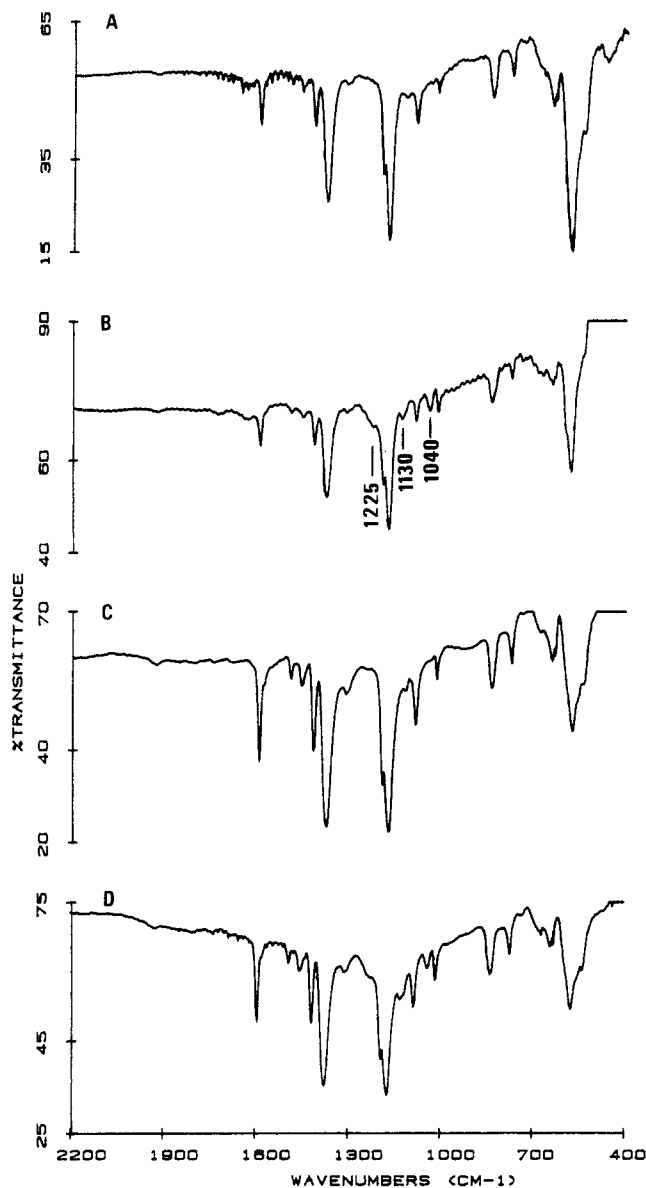


**Figure 4.** FTIR spectra of PS-SO<sub>2</sub>Cl: (A) in a KBr pellet; (B) the same spectrum in KBr after stirring the suspended polymer in a 0.5 M Na<sub>2</sub>CO<sub>3</sub>/0.5 M NaHCO<sub>3</sub> buffer (pH ~9.6) for 12 h; (C) obtained by specular reflectance (45°) as a spun-cast film (~1200 Å thick) on a glass/titanium/platinum substrate; (D) as in (C) except after soaking in buffer solution (pH 9.6) for 4 h.

The luminescence was totally quenched upon the addition of sufficient PQ<sup>2+</sup> to make the solution 2 mM in PQ<sup>2+</sup>. The quenching of luminescence was maintained even after soaking the film for 20 min in neat acetonitrile. Upon addition of 0.1 M [NEt<sub>4</sub>](ClO<sub>4</sub>), the luminescence was immediately restored, evidently because of exchange of NEt<sub>4</sub><sup>+</sup> ion for PQ<sup>2+</sup> in the film.

The workup procedure for the chlorosulfonated polystyrene<sup>12</sup> unavoidably causes a certain degree of hydrolysis. The extent of additional hydrolysis induced by the soaking procedures described here could be estimated, at least qualitatively, by IR spectroscopy. Figure 4A shows the IR spectrum of a sample of PS-SO<sub>2</sub>Cl in KBr immediately after synthesis and workup. Figure 4B is a spectrum of the same polymer in KBr but after it was stirred as a suspension in aqueous base (pH 9.6) for 12 h. The peaks at 1040 and 1130 cm<sup>-1</sup> and the shoulder at 1225 cm<sup>-1</sup> show the appearance of sodium polystyrene sulfonate, PS-SO<sub>3</sub><sup>-</sup>Na<sup>+</sup>.<sup>16</sup>

Figure 4C shows the specular reflectance IR spectrum of a sample of PS-SO<sub>2</sub>Cl cast as a film (~1550 Å thick) on a glass/titanium/platinum substrate, and Figure 4D the same film

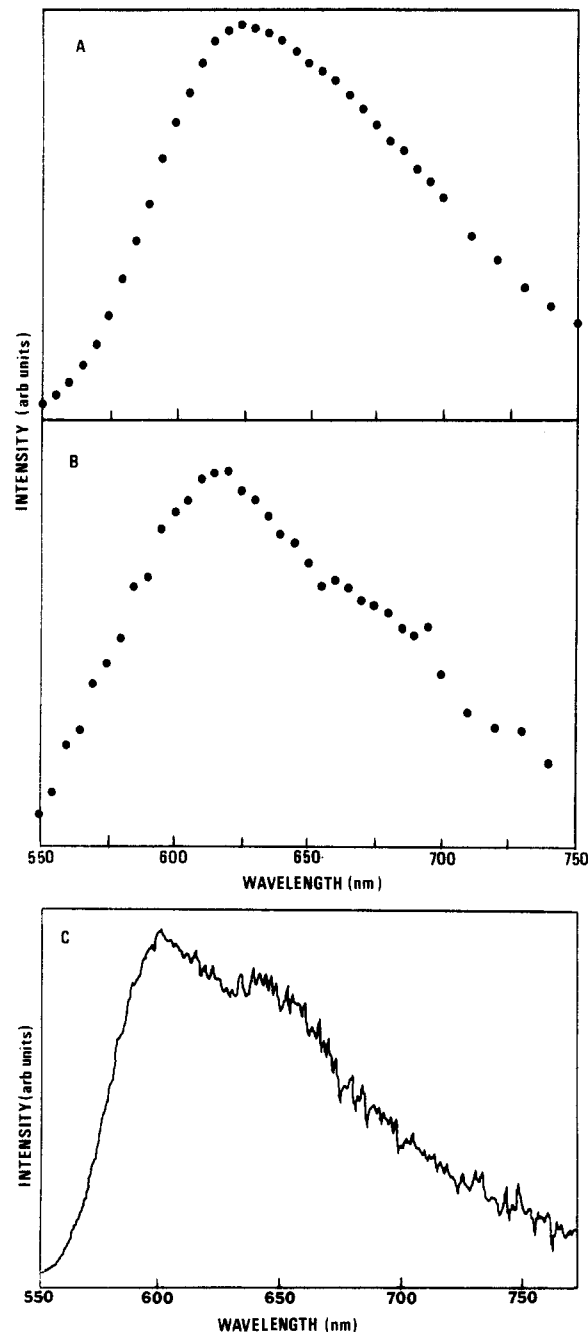


**Figure 5.** Emission spectra at 25 °C obtained following 450-nm laser excitation: (A) [(bpy)<sub>2</sub>Ru(5-NH<sub>2</sub>phen)][PF<sub>6</sub>]<sub>2</sub> monomer in 0.1 M TEAP/CH<sub>3</sub>CN; (B) PS-SO<sub>2</sub>Cl polymeric film into which [(bpy)<sub>2</sub>Ru(5-NH<sub>2</sub>phen)]<sup>2+</sup> (2 mM) had been soaked for 2 h followed by hydrolysis in 0.5 M Na<sub>2</sub>CO<sub>3</sub>/0.5 M NaHCO<sub>3</sub> for 3 h; (C) dry polymeric film at 77 K using 425-nm continuous wave excitation. The film was prepared by soaking a PS-SO<sub>2</sub>Cl film in an CH<sub>3</sub>CN solution containing the metal complex (2 mM) for 17 h and rinsing with CH<sub>3</sub>CN.

after soaking in base for 4 h. The extent of hydrolysis indicated in Figure 4B,D is comparable and, by comparing peak ratios, is <5% of the total PS-SO<sub>2</sub>Cl sites. Films having comparable properties in the photoelectrochemical experiments described later could be obtained by prehydrolysis and film formation or by hydrolysis of intact films. So that equivalent results with films formed following prehydrolysis could be obtained, it was necessary to hydrolyze the intact films for ~15 min after incorporation of the Ru complex.

**Photophysical Properties.** In Figure 5A,B are shown emission spectra for the monomer, [(bpy)<sub>2</sub>Ru(5-NH<sub>2</sub>phen)]<sup>2+</sup>, in CH<sub>3</sub>CN at room temperature, and of the sulfonamide-bound analogue, [(bpy)<sub>2</sub>Ru(5-PS-SO<sub>2</sub>NH(phen))]<sup>2+</sup>, with the polymeric film exposed to an external solution of CH<sub>3</sub>CN. The spectra were obtained by integrating the emission intensity of the transient decay

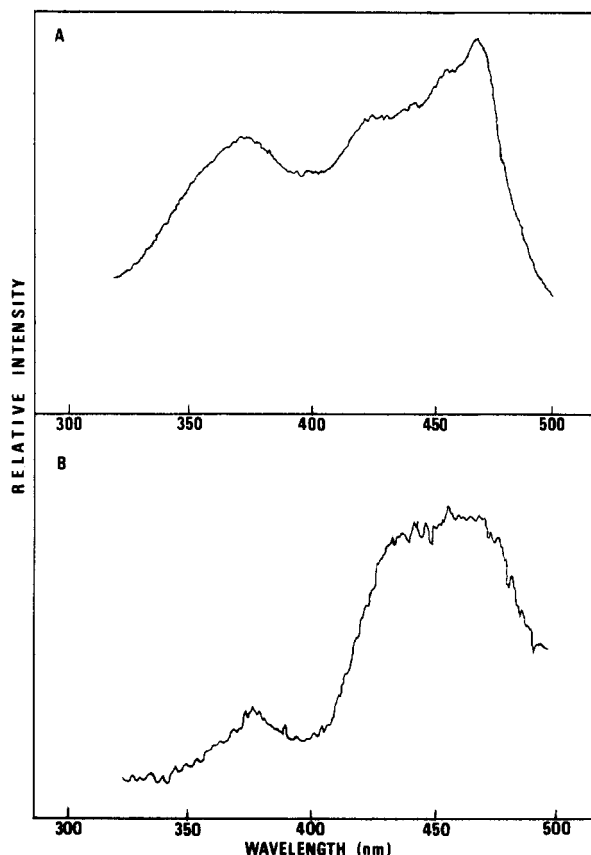


Figure 6. Excitation spectra (A) of  $[(bpy)_2Ru(5-NH_2phen)](PF_6)_2$  in 0.1 M TEAP/ $CH_3CN$  (25 °C) detected at 620 nm; (B) of the same film as in Figure 5C at 77 K detected at 630 nm.

as a function of emission wavelength excitation at 450 nm by a pulsed  $N_2$ /dye laser and are corrected for detector response. The technique is highly sensitive and allows for the acquisition of emission spectra from films containing relatively low loadings of chromophore. So that spectra from a conventional emission spectrofluorimeter could be obtained, much higher loadings were required (soaking times of hours instead of minutes). Also it was necessary to cool dry films to 77 K, as shown in Figure 5C.

There are no substantial differences between the solution and film-based emission spectra. The  $\sim 1300\text{-cm}^{-1}$  vibrational structure that appears at 77 K is common for bpy- or phen-based MLCT emitters and arises from an averaged contribution from a series of  $\nu(bpy)$  or  $\nu(phen)$  ring stretching modes.<sup>17</sup>

Excitation spectra for both the solution and film-bound complexes exposed to  $CH_3CN$  are shown in Figure 6A,B. There is a notable lack of detailed structure in the film spectrum and a decrease in relative intensity at 372 nm consistent with loss of the 5- $NH_2phen$ -based  $n \rightarrow \pi^*$  transition due to sulfonamide formation.

Emission decay within the polymeric films soaked in 0.1 M TEAP in acetonitrile is nonexponential as shown in Figure 7. Starting 20 ns after the laser pulse to avoid problems associated with light scattering, the decay data could be satisfactorily fit as the sum of two exponentials via the equation

$$I(t) = A_1 \exp(-t/\tau_1) + A_2 \exp(-t/\tau_2) \quad (8)$$

and the method of nonlinear least-squares using a Marquardt algorithm.<sup>18</sup> The best fit treatment of decay curves like that shown in Figure 7 gave  $\tau_1 (=1/k_1) = 700$  ns and  $\tau_2 (=1/k_2) = 115$  ns and  $A_2/A_1 = 3.75$  ( $A_1 = 0.04$ ,  $A_2 = 0.15$ ). Given the nature of the fitting procedure, the absolute magnitudes of the constants  $A_1$  and  $A_2$  depend on such quantities as the concentration and light absorptivity of the chromophore and the emission efficiency of the excited states, which in general vary from exper-

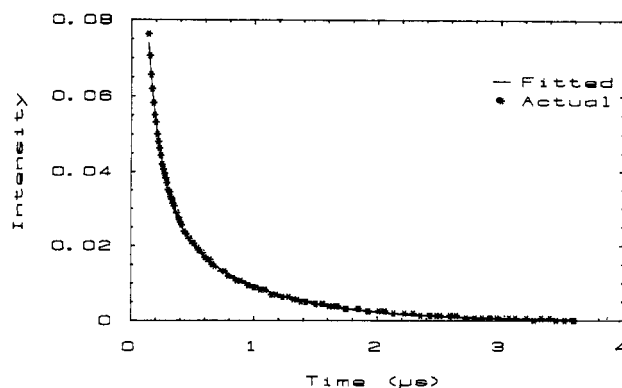


Figure 7. Time-resolved emission intensity of a  $[(bpy)_2Ru(5-PS-SO_2NH(phen))]^{2+}$ -containing film on a platinum slide in 0.1 M TEAP/ $CH_3CN$  prepared by soaking a PS- $SO_2Cl$  film in a 5 mM  $[(bpy)_2Ru(5-NH_2phen)_2](PF_6)_2/CH_3CN$  solution for 2 h and hydrolyzing in 0.5 M  $Na_2CO_3/0.5$  M  $NaHCO_3$  for 3.5 h. This corresponds to  $\sim 1\%$  loading of available  $-SO_2Cl$  sites by the metal complex. The  $CH_3CN$  solution surrounding the film was deaerated with argon. Also shown is a least-squares fit of the data at  $t > 20$  ns using the biexponential function in eq 8;  $R^2 = 0.9991$ .

iment to experiment. However, in making comparisons between experiments the ratio  $A_2/A_1$ , which is a measure of the relative amount of light emitted by the short lifetime component, is of relevance. In acetonitrile at room temperature, the MLCT excited states of  $[(bpy)_2Ru(5-NH_2phen)]^{2+}$  and  $[(bpy)_2Ru(5-N(p-SO_2C_6H_4CH_3)_2phen)]^{2+}$  decay exponentially with lifetimes of 1150 and 1800 ns, respectively.<sup>11,19</sup>

Nonexponential excited-state decay is a common feature in polymeric film and related environments.<sup>6a,20</sup> In our films in which  $[Zn(5-NH_2phen)_3]^{2+}$  and  $[(bpy)_2Ru(5-NH_2phen)]^{2+}$  are co-incorporated at a ratio of up to 2.5:1 Zn to Ru, the decay characteristics of the Ru-based MLCT excited state were essentially unchanged. The absence of a dilution effect suggests that self-quenching is not an important deactivation pathway, a conclusion that is supported by the absence of a change in lifetime when the laser intensity was decreased by a factor of 2 by using neutral density filters. When a preformed film containing bound complex was dissolved in DMSO, the deviation from single-exponential behavior was less marked but still noticeable.<sup>21</sup>

**Quenching by Added  $PQ^{2+}$ .** Because the complex containing films are weak emitters, conventional intensity quenching experiments were relatively imprecise, and the extent of quenching was monitored by integrating the area under the  $I$  vs  $t$  transient decay curves. The experiments were carried out with the films exposed to a 3-mL volume of acetonitrile containing 0.1 M TEAP with varying amounts of added  $PQ^{2+}$ , and the decay curves monitored following pulsed excitation from a  $N_2$  pumped dye laser.

Quenching studies over a wide range of  $PQ^{2+}$  concentrations reveal three distinct quenching regions. A plot of  $I_0/I$  vs  $[PQ^{2+}]$  in 0.1 M TEAP/acetonitrile in the external solution is shown in Figure 8A for a film soaked for 2 h in chromophore solution and hydrolyzed for 3.5 h. At low added  $PQ^{2+}$  ( $<0.10$  mM), a rapid quenching process occurs followed by a decrease in apparent rate as  $[PQ^{2+}]$  is increased. At high  $PQ^{2+}$  concentrations ( $\geq 3$  mM) the extent of quenching reaches a plateau past  $[PQ^{2+}] \sim 50$  mM, where no further quenching occurs and yet  $\sim 30\%$  of the initial emission intensity remains. The behavior illustrated in Figure 8A has been observed in several separate samples.

To treat our data, we have turned to an analysis that was developed to account for the intensity quenching behavior of protein-bound fluorophors exposed to solution quenchers.<sup>22</sup> In

(19) McClanahan, S. F.; Margerum, L. D., unpublished results.

(20) (a) Wheeler, J.; Thomas, J. K. *J. Phys. Chem.* **1982**, *86*, 4540. (b) Wei, S.; Gafney, H. D.; Clark, J. B.; Perette, D. J. *Chem. Phys. Lett.* **1983**, *99*, 253. (c) LeLand, B. A.; Joran, A. D.; Felker, P. M.; Hopfield, J. J.; Zewail, A. H.; Dervan, P. B. *J. Phys. Chem.* **1985**, *89*, 5571. (d) Lindsey, J. S.; Mauzerall, D. C.; Linschitz, H. *J. Am. Chem. Soc.* **1983**, *105*, 6528.

(21) McClanahan, S. F., unpublished results.

(22) Lehrer, S. S. *Biochemistry* **1971**, *10*, 3254.

(17) Caspar, J. V.; Westmoreland, T. D.; Allen, G. H.; Bradley, P. G.; Meyer, T. J.; Woodruff, W. H. *J. Am. Chem. Soc.* **1984**, *106*, 3492.

(18) Marquardt, D. W. *J. Soc. Ind. Appl. Math.* **1963**, *2*, 431.

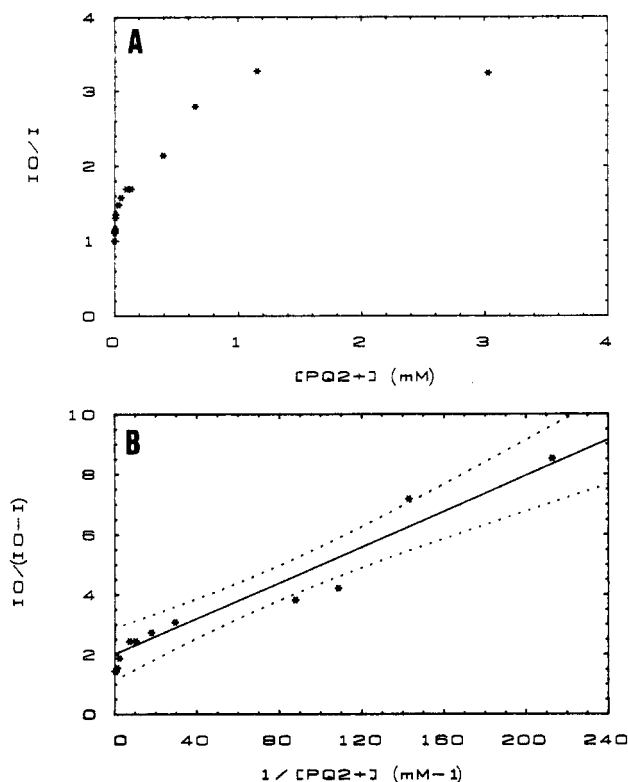


**Figure 8.** (A) Intensity quenching study of a film prepared as in Figure 7, as a function of added  $PQ^{2+}$  in the external 0.1 M TEAP- $CH_3CN$  solution. The intensity,  $I$ , was obtained as the average integrated area under 200 transient  $I$  vs  $t$  curves at the emission maximum (625 nm) beginning at 20 ns after the laser pulse to the end of significant emission following excitation at 460 nm. (B) Modified Stern-Volmer plot of the data in (A) according to eq 9. Also shown is the least-squares regression line for points where  $[PQ^{2+}] \leq 0.15$  mM, including the 95% confidence levels.

the analysis a distribution of emitting sites is assumed to exist between areas of the protein that are accessible to quencher and those that are not. If the analysis given by Lehrer is appropriate to our case, a plot of  $I_0/(I_0 - I)$  vs  $1/[PQ^{2+}]$  should yield a linear region at low  $[PQ^{2+}]$  where only the easily accessible sites are quenched. In general, for a series of sites  $i$

$$\frac{I_0}{I_0 - I} = \frac{1}{[PQ^{2+}] \sum_{i=1}^n f_i K_{SVi}} + \frac{\sum_{i=1}^n f_i K_{SVi}}{\sum_{i=1}^n f_i K_{SVi}} \quad (9)$$

where the summation is over the total number of different chromophoric sites  $i$ . In eq 9,  $f_i$  is the "maximum accessible fraction" of chromophores quenched, with a Stern-Volmer constant  $K_{SVi}$ . If the emission quantum yield and wavelength characteristics of emission for all of the sites are the same,  $f_i$  is given by the ratio of the intensity of light emitted by site  $i$  to the total light emitted:

$$f_i = I_{0i}/I_0$$

However, in general, the photophysical properties of different sites will be different, and the ratio  $I_{0i}/I_0$  is a measure only of the fraction of light emitted by site  $i$  and not a measure of the total fraction of sites that are  $i$ .

Shown in Figure 8B is a plot of  $I_0/(I_0 - I)$  vs  $1/[PQ^{2+}]$  for the same data shown in Figure 8A at low  $[PQ^{2+}]$ . Although the scatter in the data at such low quencher concentrations (4–60  $\mu\text{M}$ ) is necessarily high, a consistent linear trend has been observed in a number of independent experiments. The linear region is maintained to  $[PQ^{2+}] \sim 0.12$  mM, after which the contribution from the slower quenching process becomes important. Extrapolation of the data in Figure 8B to the intercept at  $1/[PQ^{2+}] = 0$  in the region of low quencher concentration gives an intercept

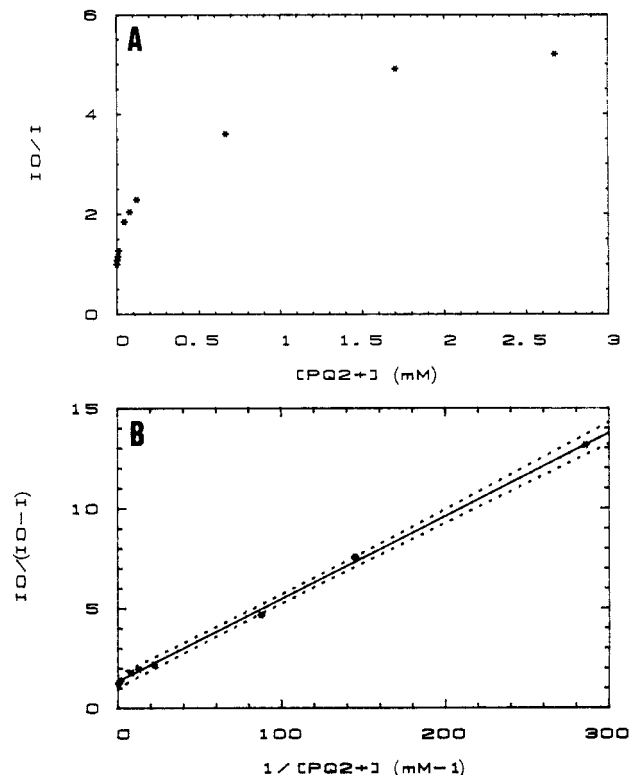


**Figure 9.** (A) Intensity quenching study of a film prepared under identical conditions as described in Figure 8 but in a solution 0.1 M in TEAP and 0.05 M in TEOA. (B) Modified Stern-Volmer plot of the data shown in (A). Also shown is the least-squares regression line for points where  $[PQ^{2+}] \leq 0.15$  mM and the 95% confidence limits.

of 2.0 and a slope of 0.030  $\text{mM}^{-1}$ . If it is assumed that quenching in this fast-quenching region arises through quenching of a single type of site, the intercept to slope ratio gives  $K_{SV(\text{fast})} = 6.7 \times 10^4 \text{ M}^{-1}$ . From the inverse of the intercept, the fraction of light emitted by the sites that are rapidly quenched is  $f_{\text{fast}} \sim 0.50$ .

From the intercept of the linear region, a value of  $I = 1.83$  can be calculated, which corresponds to the remaining light intensity that is emitted by sites not readily accessible to the quencher. The value of  $I$  so obtained provides an estimate for the initial emitted intensity  $I_{0i}$  for the sites that are more slowly quenched. On the basis of this value of  $I_{0i}$ , a plot similar to that shown in Figure 8B can be constructed for the region where the quencher concentration lies between 0.6 and 3 mM. At these concentrations, emission from the rapidly quenched sites is negligible. The plot constructed over the higher concentration range in  $PQ^{2+}$  is linear, but because of the uncertainties involved in the data and the treatment only an estimate of  $K_{SV(\text{slow})} \sim 3 \times 10^3 \text{ M}^{-1}$  could be obtained.

The results of experiments carried out on films prepared in an identical manner except with 0.05 mM triethanolamine [ $N(C_2H_4OH)_3$ ] added to the external solution are shown in Figure 9A as a plot of  $I_0/I$  vs  $[PQ^{2+}]$ . In the presence of TEOA and with or without added  $[NEt_4](ClO_4)$  at 0.1 M, a fast-quenching region is again observed at  $[PQ^{2+}] \leq 0.15$  mM followed by a slower quenching region from  $[PQ^{2+}] = 0.15$  to  $\sim 2$  mM. At higher  $[PQ^{2+}]$  the extent of quenching levels off. Qualitatively, the addition of TEOA appears to increase the extent of quenching in the fast-quenching region.

The importance of added TEOA lies in its role as reductive scavenger in the photocurrent measurements, which are the basis for the second paper in this series.<sup>14</sup> A plot of  $I_0/(I_0 - I)$  vs  $1/[PQ^{2+}]$  for the film exposed to an external solution containing both TEAP and TEOA is shown in Figure 9B. There is a considerable decrease in scatter in the data compared to the data in Figure 8B. From the intercept (1.34) and slope (0.041  $\text{mM}^{-1}$ ) of the linear region,  $K_{SV(\text{fast})} = 3.2 \times 10^4 \text{ M}^{-1}$  and  $f_{\text{fast}} = 0.74$  under these conditions.

The MLCT excited state of the monomeric complex  $[(bpy)_2Ru(5-NH_2phen)]^{2+}$  is quenched by  $PQ^{2+}$  under the same



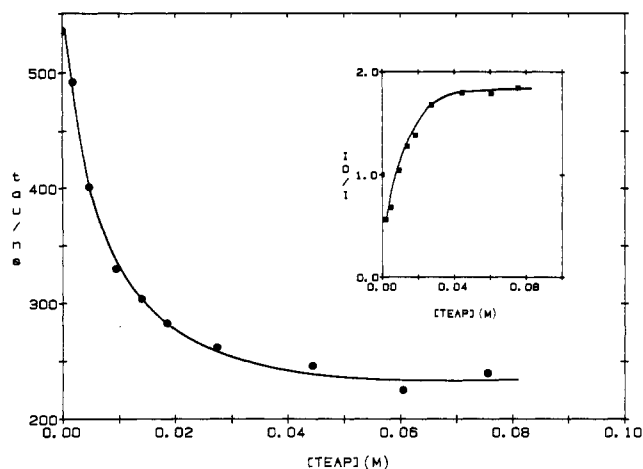


**Figure 10.** Lifetime and intensity quenching data at the emission maximum of 620 nm for a film prepared as in Figures 7–9 in the presence of 1.1 mM  $PQ^{2+}$  as a function of added TEAP. The exciting wavelength was 450 nm.

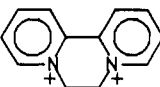
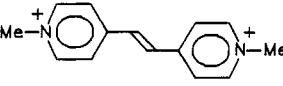
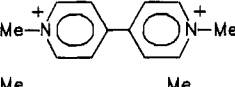
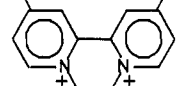
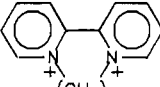
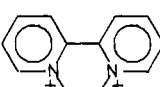
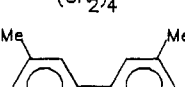
conditions in  $CH_3CN$  solution<sup>19</sup> with  $K_{SV} = 3.2 \times 10^3 M^{-1}$ . By using  $\tau = 1150$  ns,<sup>11</sup>  $k_q = 2.8 \times 10^9 M^{-1} s^{-1}$ , which is within a factor of 10 of the diffusion-controlled limit in  $CH_3CN$ . The most obvious explanation for Stern–Volmer constants for film-based quenching that appear to exceed the diffusion-controlled limit is that under the conditions of the experiment  $PQ^{2+}$  is concentrated within the film compared to bulk solution and that the partition constant,  $K_p = [PQ^{2+}]_{film}/[PQ^{2+}]_{soln}$ , is greater than unity.

We attempted to obtain an independent estimate of  $K_p$  by an electrochemical experiment. In the experiment a hydrolyzed  $PS-SO_2Cl$  film on an electrode was soaked in an acetonitrile solution 2 mM in  $PQ^{2+}$  and transferred to a clean 0.1 M TEAP solution to obtain the cyclic voltammogram of the incorporated  $PQ^{2+}/^+$  couple. From the area under the wave on a first scan and with the density of the film  $\sim 1$  g/cm<sup>3</sup>, we estimate that  $K_p \sim 10^2$ . Using  $K_p = 10^2$  and  $\tau = 700$ – $100$  ns as the range in lifetimes for the film-based excited states gives  $k_{q(fast)} \approx 9.7 \times 10^8$ – $6.8 \times 10^9 M^{-1} s^{-1}$ . Although a number of factors dictate the magnitude of  $k_q$ , the fact that the film-based value is within a factor of 10 of the solution value is notable. Decreases between solution and film-based diffusion coefficients of up to  $10^5$  have been observed for other electrochemical redox couples in related films.<sup>23</sup>

The kinetics of the fast-quenching process are relatively independent of added TEAP, but the slower process has a strong, remarkable dependence on TEAP as shown in Figure 10 by the dependence of the lifetime and  $I_0/I$  ratios on added TEAP in the presence of sufficient  $PQ^{2+}$  (1.1 mM) that the rapid quenching process is complete and not interfering. At added  $[TEAP] = 0$ , about 50% of the emitted light remains unquenched. The residual emission retains its nonexponential character with the decay parameters for the two-component fit from eq 8 being 590 and 154 ns. The similarity between the kinetic decay parameters obtained in the absence of any added  $PQ^{2+}$  (Table I) and those obtained in the presence of 1.1 mM  $PQ^{2+}$  shows that the excited-state sites giving rise to the two different quenching processes have similar photophysical properties.

From the data in Figure 10, the process involving slow quenching by  $PQ^{2+}$  essentially does not occur in the absence of added TEAP. However, as TEAP is added, both the emitted light intensity and its lifetime decrease. As increasing amounts of TEAP are added, both  $\tau_1$  and  $\tau_2$  in eq 8 decrease in a parallel fashion. The lifetime data displayed in Figure 10 utilize the slower component  $\tau_1$  from the fitting procedure based on eq 8. It is apparent from the data that the slow-quenching process is highly dependent on added TEAP up to a level of  $\approx 0.05$  M, past which no further quenching is observed. From the ratio  $I_0/I$  with  $[TEAP] > 0.5$  M, where the slow-quenching step is complete, a considerable fraction of the emitting sites still remains unquenched at this point.

**TABLE II:  $K_{SV}$  Values Obtained by Photocurrent Measurements in  $CH_3CN$**

quencher	$E_{1/2}(2+/+)$ , V <sup>a</sup>	$K_{SV}$ , <sup>b</sup> M <sup>-1</sup>
	-0.44	$6 \times 10^4$
	-0.50	$5 \times 10^4$
	-0.51	$1.2 \times 10^5$
	-0.55	60
	-0.64	20
	-0.71	2
	-0.84	c

<sup>a</sup>Reduction potentials vs saturated sodium chloride calomel electrode. For comparison  $E_{1/2} = +310$  mV for ferricinium/ferrocene under similar conditions (0.1 M  $KPF_6$ ,  $CH_3CN$ ). <sup>b</sup>From photocurrent measurements in either 0.1 M TEAP or 0.1 M  $NH_4PF_6$ ,  $CH_3CN$ .  $NH_4PF_6$  was used, where necessary, to achieve sufficient quencher solubility. <sup>c</sup>No photocurrent detected.

From the extent of quenching at  $[TEAP] > 0.05$  M, it can be estimated that of the fraction of light emitted by the sites remaining after rapid quenching,  $\sim 50\%$  is emitted by sites that undergo slow quenching and the remainder from sites that are not accessible to the quencher. From lifetime results under conditions where further added  $PQ^{2+}$  or TEAP has no effect, the residual, unquenchable excited states still undergo nonexponential decay but with  $\tau$  values for both components in the fitting procedure by using eq 8 which are considerably shortened,  $\tau_1 \approx 250$  ns,  $\tau_2 \approx 65$  ns, and  $A_2/A_1 = 10$ .

The emission intensity data show that there is actually a slight increase in emitted intensity following the addition of the first aliquot of TEAP (inset in Figure 10). The effect is apparently a medium effect. It may arise from structural changes in the films arising from the incorporation of TEAP, which has the effect of enhancing emission from all of the emitting sites. However, any environmental change induced by TEAP has the ultimate effect of inducing quenching by  $PQ^{2+}$  as the level of added TEAP is increased.

**Kinetic Quenching of the Excited States. Estimation of Excited-State Redox Potentials.** In the second paper in this series,<sup>14</sup> the results of an extensive series of photocurrent measurements are described in which the photocurrents are induced in the presence of added  $PQ^{2+}$  and the reductive scavenger TEOA. In that work it is shown that at constant light intensity and constant added  $[TEOA]$  the inverse of the observed photocurrent varies with  $[PQ^{2+}]$  as

$$i_{hv}^{-1} = (1 + 1/K_{SV}[PQ^{2+}])C \quad (10)$$

where  $C$  is a constant. From the slope to intercept ratio it is possible to evaluate  $K_{SV}$ . The photocurrent measurements thus provides a relatively straightforward means for investigating quenching dynamics within the films.



We have carried out a series of such measurements based on the pyridinium quenchers listed in Table II. Although the techniques used and the interpretation of data for  $PQ^{2+}$  as quencher will be discussed in detail in the second paper, the results obtained are most conveniently presented here. In previous work of this kind, experimentally derived quenching rate constants for a similar set of quenchers was utilized to estimate excited-state redox potentials for  $Ru(bpy)_3^{2+}$  in acetonitrile solution.<sup>24</sup> The basis for the approach lies in the application of a kinetic analysis first presented by Rehm and Weller,<sup>25</sup> the utilization of electron-transfer theory, and the experimental variation of  $k_q$  with the free energy change for the quenching step.

Direct application of the kinetic quenching technique to the film experiments based on photocurrent measurements and eq 10 is not possible. The problem lies in the somewhat equivocal situation created by the existence of both slow- and fast-quenching sites, the nonexponential nature of excited-state decay in the films, and possible variations in the partition constants ( $K_p$ ) for the various quenchers. A simplification arises from the fact that as shown in the second paper in the series, only the fast quenching component contributes to the observed photocurrents. Even given the remaining complications it seems clear from the dramatic falloff in  $K_{SV}$  as  $E_{1/2}$  for the quencher couple falls, that the potential for the film based excited-state couple  $[(bpy)_2Ru(5-NH(SO_2-PS)phen)]^{3+}/[(bpy)_2Ru(5-NH(SO_2-PS)phen)]^{2+}$  lies between -0.50 and -0.70 V. This value is within striking distance of the value of  $E^0 = -0.81$  V vs SCE obtained for the  $[Ru(bpy)_3]^{3+}/[Ru(bpy)_3]^{2+}$  couple under the same conditions in  $CH_3CN$  solution.<sup>24</sup>

## Discussion

**Physical and Chemical State of the Chromophore.** The available evidence suggests that following the soaking procedure for the incorporation of  $[(bpy)_2Ru(5-NH_2phen)]^{2+}$  into preformed films of chlorosulfonated polystyrene (PS- $SO_2Cl$ ), the chromophore is chemically attached to the polymer via sulfonamide bond formation. The question of whether the chemical linkage is via one,  $[(bpy)_2Ru(5-NH(SO_2-PS)phen)]^{2+}$ , or two,  $[(bpy)_2Ru(5-N(SO_2-PS)_2phen)]^{2+}$ , sulfonamide links or a combination of the two remains unresolved.

The results of the emission, excitation, and absorption experiments described here suggest that, at least in a general sense, the low-energy MLCT electronic structure of the chromophore is maintained in the films. In addition, based on the results of the photocurrent measurements in Table II, the redox potential of the  $[(bpy)_2Ru(5-NH(SO_2-PS)phen)]^{3+}/[(bpy)_2Ru(5-NH(SO_2-PS)phen)]^{2+}$  couple is less than or comparable to the potential for the  $[Ru(bpy)_3]^{3+}/[Ru(bpy)_3]^{2+}$  couple in acetonitrile, showing that the thermodynamic reducing ability of the excited state is also maintained in the films.

Although the properties of the film-based excited state are superficially comparable to monomeric analogues in solution, the lifetime experiments, which by their nature are relatively precise, reveal that the film environment has a significant impact on the decay characteristics of the MLCT excited state. In the film environment the excited-state lifetime is shortened and excited-state decay becomes nonexponential. That the film-based environment has a significant impact on excited-state properties is hardly surprising given the following: (1) The possible existence of two electronically nonequivalent sites based on the formation of mono- and disulfonamide links to the polymeric backbone of the films. Changes in both nonchromophoric ligands and in substituents on the chromophoric ligand are known to influence excited-state lifetimes.<sup>14,26</sup> (2) The fact that Ru-based MLCT excited-state decay is, in general, dependent on both radiative and nonradiative decay from the lowest MLCT state(s) and, also, on thermal activation to and subsequent decay from low-lying dd

states.<sup>26,27</sup> Both types of processes are known to be medium dependent. (3) The appearance of either self-quenching,<sup>28</sup> possibly via  $2[(bpy)_2Ru(5-NH(SO_2-PS)phen)]^{2+} \rightarrow [(bpy)_2Ru^{III}(5-NH(SO_2-PS)phen)]^{3+} + [(bpy)_2Ru^{II}(5-NH(SO_2-PS)phen^{\bullet-})]^+$ , or quenching of the excited state at the electrode. (4) The lifetime quenching evidence for three different emitting sites in the films. (5) The possible role of localized, relatively slow dipole reorientations that occur on the same time scale as excited-state decay.<sup>29</sup>

The results of the dilution experiment based on  $[Zn(5-NH_2phen)_3]^{2+}$  suggest that self-quenching does not play an important role. Quenching by the electrode can also be ruled out since the same lifetime characteristics are obtained for films prepared on glass slides as on Pt or glassy carbon electrodes.

Localized environmental dipole effects do appear to play a role as evidenced by a time-resolved experiment in which it was observed that the emission maximum is time dependent at room temperature, changing from  $\sim 605$  nm at 20 ns to  $\sim 620$  nm at 100 ns after excitation at 480 nm.<sup>30</sup> In addition, a decrease in the extent of nonexponential lifetime behavior is observed when the polymer is dissolved in DMSO, where the rate of local dipole reorientations is enhanced relative to the film environment, and at 77 K, where dipole reorientations are frozen on the time scale for excited-state decay. The situation in the films may be analogous to that of the glass to fluid transition region in, for example, 4:1 (V:V) ethanol-methanol. Temperature-dependent lifetime studies of similar chromophores in the glass to fluid transition region for this medium have shown that complex decay kinetics appear when the reorientation of solvent dipoles in the surrounding medium occurs on the same time scale as excited-state decay.<sup>29</sup> Such effects may also be operative in the viscous environment of the polymeric films at room temperature. In any case, we have found that satisfactory fits of the lifetime data can be obtained by using the relatively simple biexponential decay function in eq 8.

The quenching experiments with  $PQ^{2+}$  provide direct evidence that following the hydrolysis step, the chromophore occupies three distinctly different sites within the films. Site 1, whose existence depends upon the hydrolysis step, accounts for  $\sim 50\%$  of the emitted light intensity. Quenching at site 1 is rapid and relatively unaffected by added  $[NEt_4](ClO_4)$ . The appearance of Stern-Volmer kinetics shows that quenching by  $PQ^{2+}$  is diffusional rather than static in nature. In the presence of 0.05 M added TEOA, the fraction of emitted light from the rapidly quenched sites rises to  $\sim 75\%$  at the expense of both the slowly quenched and non-quenched sites. The large  $K_{SV}$  value of  $6.7 \times 10^4 M^{-1}$  ( $3.2 \times 10^4 M^{-1}$  in the presence of 0.05 M added TEOA) for the rapid quenching process provides evidence that  $PQ^{2+}$  is concentrated within the hydrolyzed films by ion exchange. The concentrating effect of the films was verified by electrochemical experiments which gave  $K_p \sim 10^2$  for the partition coefficient for  $PQ^{2+}$  within the film.

Partial hydrolysis is required for quenching to occur and, once hydrolyzed, quenching is rapid in the films. The rate constant for quenching is comparable to solution values. However, from the electrochemical result in Figure 3, partial hydrolysis has, at best, a small effect on the transport of the  $PQ^{2+/+}$  couple through the films. By inference, long-range translational channels must

(24) Bock, C. R.; Conner, J. A.; Gutierrez, A. R.; Meyer, T. J.; Whitten, D. G.; Sullivan, B. P.; Nagle, J. K. *J. Am. Chem. Soc.* **1979**, *101*, 4815.  
(25) (a) Rehm, D.; Weller, A. *Ber. Bunsen-Ges. Phys. Chem.* **1969**, *73*, 834. (b) Rehm, D.; Weller, A. *Isr. J. Chem.* **1970**, *8*, 259.

(26) (a) Meyer, T. J. *Pure Appl. Chem.* **1986**, *58*, 1193. (b) Juris, A.; Balzani, V.; Barigelli, F.; Campagna, S.; Belser, P.; von Zelewsky. *Coord. Chem. Rev.* **1988**, *84*, 85.

(27) Calvert, J. M.; Caspar, J. V.; Binstead, R. A.; Westmoreland, T. D.; Meyer, T. J. *J. Am. Chem. Soc.* **1982**, *104*, 6620.

(28) (a) Kelder, S.; Rabani, J. *J. Phys. Chem.* **1981**, *85*, 1637. (b) Furue, M.; Kuroda, N.; Nozakura, S.-I., *Chem. Lett.* **1986**, 1209. (c) Baxendale, J. H.; Rodgers, M. A. J. *Chem. Phys. Lett.* **1980**, *72*, 424. (d) Lachish, U.; Ottolenghi, M.; Rabani, J. *J. Am. Chem. Soc.* **1977**, *99*, 8062.

(29) (a) Lumpkin, R. S.; Meyer, T. J. *J. Phys. Chem.* **1986**, *90*, 5307. (b) Danielson, E.; Lumpkin, R. S.; Meyer, T. J. *J. Phys. Chem.* **1987**, *91*, 1305. (c) Kitamura, N.; Kim, M.-B.; Kawanishi, Y.; Obata, R.; Tazuke, S. *J. Phys. Chem.* **1986**, *90*, 1488. (d) Milder, S. J.; Gold; Kliger, D. S. *J. Phys. Chem.* **1986**, *90*, 548.

(30) Surridge, N. A.; Danielson, E.; Meyer, T. J., manuscript in preparation.

exist within the films for the  $PQ^{2+/+}$  couple before the films are hydrolyzed, but these channels are not effective in bringing  $PQ^{2+}$  to the chromophoric sites.

The collection of facts available for the fast-quenching process provides the basis for a relatively detailed kinetic and structural model for what occurs at site 1. The role of the hydrolysis step may be to create "ion-exchange incursion channels" that penetrate from the translational channels into the hydrophobic bulk of the films where the majority of the chromophores resides. In this model the incursion channels provide a basis for the diffusion of the  $PQ^{2+/+}$  couple from the translational channels to the chromophore.

With this interpretation of the results, the fast-quenching process must occur at those chromophoric sites that lie at or sufficiently near the ion incursion channels that rapid, diffusional quenching by  $PQ^{2+}$  can occur. Even though the chromophoric sites are held near the ion channels and  $PQ^{2+}$  may be concentrated within them, the quenching process is diffusional and relies on the mobility of  $PQ^{2+}$  through the films and into the incursion channels.

The majority of  $-SO_2Cl$  sites within the films remain unhydrolyzed and hydrophobic in character. Partial hydrolysis creates a basis for the appearance of separated ion-channel and hydrophobic domains within the films, as has been reported, for example, for the sulfonate-based perfluorinated polyether, Nafion.<sup>31</sup>  $PQ^{2+}$  is concentrated within the films, presumably largely in the translational channels and in the ion incursion channels.

The second site for the chromophore in the films, site 2, accounts for ~20–30% of the emitted light intensity and is quenched relatively slowly by  $PQ^{2+}$  and then only in the presence of added  $[NEt_4](ClO_4)$ . Although the quenching dynamics are dramatically different between sites 1 and 2, their excited-state decay properties are similar (eq 8) with  $\tau_1 = 700$  ns,  $\tau_2 = 115$  ns, and  $A_2/A_1 = 3.75$  for site 1 and  $\tau_1 = 590$  ns,  $\tau_2 = 154$  ns, and  $A_2/A_1 = 2.83$  for site 2. The similarities in photophysical properties suggest that the two sites have similar electronic structures and surrounding environments.

Presumably, the chromophores at site 2 are removed from the ion incursion channels and are located further into the hydrophobic interior of the films. As in the unhydrolyzed films, diffusion of the  $PQ^{2+/+}$  couple within this region is probably slow, and the concentration of  $PQ^{2+}$  is likely to be considerably lower than in the ion incursion channels. The combined effect is that oxidative quenching is not competitive with excited-state decay. The addition of either triethanolamine or  $[NEt_4](ClO_4)$  provides a basis for quenching at site 2. Given its ability to act as an ion carrier across membranes, added TEAP may open ion migration channels that allow  $PQ^{2+}$  to diffuse into and through the hydrophobic region at rates sufficient to quench the excited state before it decays.

From the results of the Stern-Volmer experiments, the addition of TEOA to the external solution converts site 2 sites into site 1 sites. Presumably, TEOA enters and swells the polymeric matrix, increasing the domain where diffusion by  $PQ^{2+}$  is sufficiently rapid to obtain quenching.

Even at high concentrations of added  $PQ^{2+}$  with 0.1 M added TEAP, a certain fraction of the chromophores, those that occupy site 3, remain unquenched. Emission from the chromophores in site 3 accounts for 20–30% of the total emission intensity. The photophysical characteristics are significantly different from those at sites 1 or 2 with  $\tau_1 = 250$  ns,  $\tau_2 = 65$  ns, and  $A_2/A_1 = 10$ . Comparison of the residual emission under quenching conditions in the presence and absence of TEOA (Figures 9B and 8B) suggests that at 0.05 M added TEOA, at least partial quenching of the excited states that occupy site 3 is induced.

We presume that at what we describe as site 3 the chromophores are located in the hydrophobic region of the film perhaps in regions

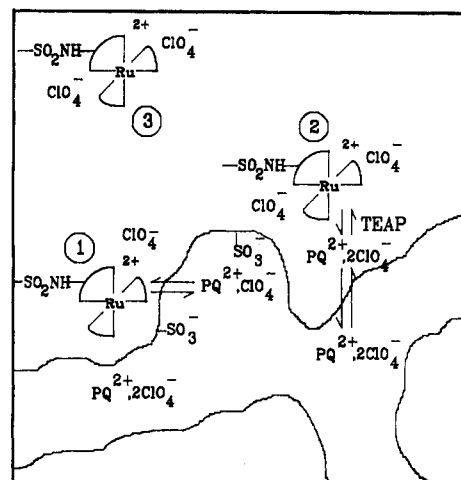


Figure 11. Structural model for the chromophore-quencher apparatus illustrating the existence of the three different sites for the chromophore and the ion-exchange incursion channels within a microdomain of the polymeric film.

of high local crystallinity, where diffusion is slow. Partial quenching with added TEOA may be an additional consequence of film swelling, which creates access to additional excited states by  $PQ^{2+}$ . Given the presumed environment at site 3, the decrease in lifetime is surprising. For related MLCT excited states in polymeric films, frozen solutions, or glasses,<sup>29</sup> the surrounding dipoles of the medium are frozen on the lifetime of the excited state and enhanced lifetimes are normally observed. The increase in lifetime has its origin in an increased energy gap between the excited and ground states which decreases the rate of nonradiative decay as predicted by the energy gap law.<sup>26,32</sup> One possibility is that an additional decay mechanism or mechanisms may exist in the crystalline regions of the films, perhaps arising from self-quenching or from entrapped  $O_2$ .

The evidence presented here shows unequivocally, at least in a physical sense, that distinctly different sites exist for the chromophore in the partly hydrolyzed PS- $SO_2Cl$  films. Evidence for interior inhomogeneities has been obtained in other film-based systems including poly(*N*-vinyl-2-methylimidazole), which contains both hydrophilic and hydrophobic groups,<sup>33</sup> in pure polystyrene sulfonate containing ion-exchanged complexes,<sup>6e</sup> and in Nafion, where direct evidence for the occupation of three distinct domains by polypyridyl complexes of Ru has been obtained by electrochemical measurements.<sup>31b</sup>

**Structure within the Film.** The results of the photophysical and quenching studies lead to a relatively detailed, physically based model for the structure of the assembled molecular level chromophore-quencher apparatus within partly hydrolyzed PS- $SO_2Cl$  films. An attempt to illustrate that structure based on the available experimental facts is made in Figure 11. The following features are incorporated in Figure 11: (1)  $PQ^{2+}$  is concentrated within the films compared to bulk solution either as the  $PF_6^-$  salt or, as illustrated here, in the presence of TEAP as the  $ClO_4^-$  salt. Although the extent of hydrolysis is low, it results in ion incursion channels which provide a relatively facile conduit between excited states that lie near the channels and the extended translational channels that permit  $PQ^{2+/+}$  transport to the electrode. (2) The appearance of the fast-quenching component, which we have termed site 1, also depends upon the hydrolysis step. Site 1 sites

(31) (a) Yeager, H. L.; Steck, A. *J. Electrochem. Soc.* **1981**, *128*, 1880. (b) Vining, W. J.; Meyer, T. J. *J. Electroanal. Chem.* **1987**, *237*, 191. (c) Hsu, W. Y.; Gierke, T. D. *Macromolecules* **1982**, *15*, 101. (d) Szeutirmay, M. N.; Prieto, N. W.; Martin, C. R. *J. Phys. Chem.* **1985**, *89*, 3017. (e) Rubenstein, I.; Bard, A. J. *J. Am. Chem. Soc.* **1981**, *103*, 5007. (f) Martin, C. R.; Rubenstein, I.; Bard, A. J. *J. Am. Chem. Soc.* **1982**, *104*, 4817. (g) Oyama, N.; Anson, F. C. *J. Electrochem. Soc.* **1980**, *127*, 247.

(32) (a) Englman, R.; Jortner, J. *Mol. Phys.* **1970**, *18*, 145. (b) Henry, B. R.; Siebrand, W. *Organic Molecular Photophysics*; J. B. Birks: London, 1973; Vol. 1, Chapter 4. (c) Fong, F. K. *Top. Appl. Phys.* **1976**, *15*. (d) Avouris, P.; Gelbart, W. M.; El-Sayed, M. A. *Chem. Rev.* **1977**, *77*, 793. (e) Freed, K. F. *Acc. Chem. Res.* **1978**, *11*, 74. (f) Lim, E. C. *Excited States*; Academic: New York, 1979. (g) Lin, S. H. *Radiationless Transitions*; Academic: New York, 1980. (h) Heller, E. J.; Brown, R. C. *J. Chem. Phys.* **1983**, *79*, 3336. (i) Kober, E. M.; Caspar, J. V.; Lumpkin, R. S.; Meyer, T. J. *J. Phys. Chem.* **1986**, *90*, 3722.

(33) Montgomery, D. D.; Anson, F. C. *J. Am. Chem. Soc.* **1985**, *107*, 3431.

probably line the ion incursion channels where migration of  $PQ^{2+}$  and diffusional quenching are both rapid. One effect of added TEOA is to increase the fraction of chromophores available to  $PQ^{2+}$  in this region by swelling the polymeric matrix. (3) The slow-quenching component at site 2 is buried within the hydrophobic, unhydrolyzed portion of the film where the concentration of  $[PQ](ClO_4)_2$  is low and diffusion slow. The addition of  $[NEt_4](ClO_4)$  apparently enhances the rate of ionic diffusion by  $PQ^{2+}$  in this region, and excited-state quenching, although slow, does occur. (4) Those sites that are unquenchable are shown as being deeply buried within the hydrophobic region. They may lie in domains of relatively high local crystallinity where diffusion of  $PQ^{2+}$  is slow on the time scale for the excited-state decay.

**Acknowledgment.** We acknowledge support of this research from the Department of Energy under Grant No. DE-ASO5-78ER06034.

**Registry No.**  $[(bpy)_2Ru(5-NH_2phen)]^{2+}$ , 84537-85-9;  $[(bpy)_2Ru(5-N(p-SO_2C_6H_4CH_3)_2phen)]^{2+}$ , 117024-07-4; 5-N( $p-SO_2C_6H_4CH_3$ )<sub>2</sub>phen, 116996-87-3; 6,7-dihydrodipyrido[1,2-a:2',1'-C]pyrazinedium, 2764-72-9; (*E*)-bis[1-methylpyridinium]-4,4'-(1,2-ethenediyl), 46740-72-1; 1,1'-dimethyl-4,4'-bipyridinium, 4685-14-7; 6,7-dihydro-2,11-dimethyldipyrido[1,2-a:2',1'-C]pyrazinedium, 16651-71-1; 7,8-dihydro-6H-dipyrido[1,2-a:2',1'-C][1,4]diazepinedium, 7325-63-5; 6,7,8,9-tetrahydrodipyrido[1,2-a:2',1'-C][1,4]diazocinedium, 16651-68-6; 7,8-dihydro-2,12-dimethyl-6H-dipyrido[1,2-a:2',1'-C][1,4]diazepinedium, 16651-74-4.

## Photoeffects in Thin-Film Molecular-Level Chromophore-Quencher Assemblies. 2. Photoelectrochemistry

Nigel A. Surridge, Joseph T. Hupp, Stephen F. McClanahan, Sharon Gould, and Thomas J. Meyer\*

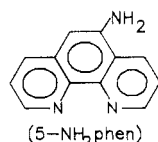
Department of Chemistry, The University of North Carolina, Chapel Hill, North Carolina 27599-3290

(Received: June 1, 1987; In Final Form: June 22, 1988)

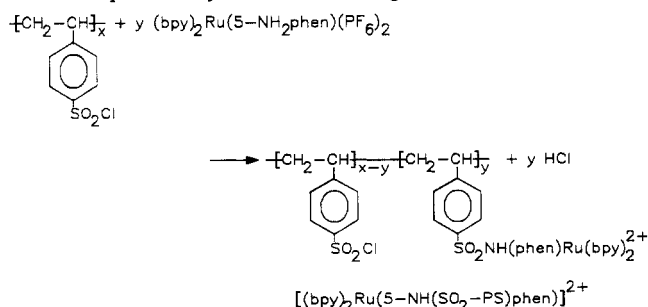
Photocurrents appear upon visible photolysis of thin films of chlorosulfonated polystyrene  $[-CH_2CH(p-C_6H_4SO_2Cl)]_x$ ;  $PS-SO_2Cl$ ) containing the chemically attached chromophore  $[(bpy)_2Ru(5-NH_2phen)](PF_6)_2$  ( $bpy$  is 2,2'-bipyridine, 5- $NH_2phen$  is 5-amino-1,10-phenanthroline). The chemical attachment is by sulfonamide binding. The photocurrents arise following oxidative quenching of the metal-to-ligand charge-transfer excited state(s) of the complex by paraquat ( $PQ^{2+}$ ) in the presence of the reductive scavenger TEOA, triethanolamine. A kinetic model has been derived that accounts for variations in photocurrent with light intensity and  $[PQ^{2+}]$  or  $[TEOA]$  in the external solution. Comparisons with earlier quenching studies obtained by laser flash photolysis show that only a fraction of the chromophores in the film contribute to the photocurrent. The efficiency of photocurrent production depends upon the concentration gradient of the chromophore. It rises initially as the chromophore content increases but falls dramatically in films where the chromophore has reached the electrode-film interface. Under maximal conditions the per photon absorbed quantum yield for photocurrent production reaches 0.14, 0.18 with 0.1 M isopropyl alcohol added.

### Introduction

In previous papers,<sup>1-3</sup> the preparation and characterization of thin polymeric films of chlorosulfonated polystyrene ( $PS-SO_2Cl$ ) were described in which the metal-to-ligand charge-transfer (MLCT) chromophore  $[(bpy)_2Ru(5-NH_2phen)]^{2+}$  ( $bpy$  is 2,2'-bipyridine; 5- $NH_2phen$  is 5-amino-1,10-phenanthroline)

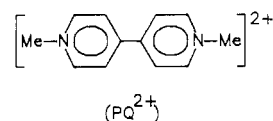


was incorporated by chemical binding:



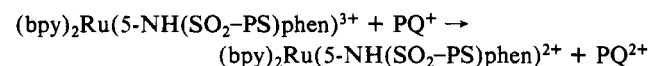
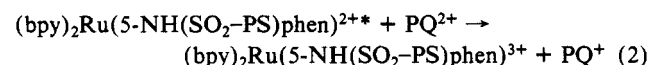
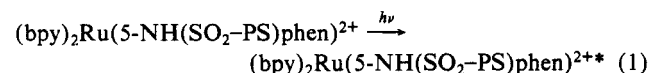
From the results of a series of photophysical and quenching studies

in the presence of the oxidative quencher  $PQ^{2+}$  (paraquat)<sup>1</sup>



a number of conclusions were reached concerning the physical structure of the resulting films: (1) Following partial hydrolysis, which converts <5% of the unreacted  $-SO_2Cl$  sites into  $-SO_3^-$  ion-exchange sites,  $PQ^{2+}$  is concentrated within the films. (2) Partial hydrolysis appears to create ion-exchange incursion channels that allow  $PQ^{2+}$  to reach and quench a high percentage of the chromophoric sites. (3) Following the hydrolysis step, the Ru-based chromophore occupies three distinctly different chemical sites. The first site is near the ion-exchange incursion channels where rapid quenching by  $PQ^{2+}$  occurs. The second is in a hydrophobic region where relatively slow quenching occurs and then only with added  $[NEt_4](ClO_4)$  as an ion carrier. The third site remains unquenched even at high quencher concentrations and may be in the hydrophobic region in a domain of relatively high local crystallinity.

As constituted, the films contain a chromophore-quencher apparatus, reactions 1 and 2, which has been used frequently in



(1) Surridge, N. A.; McClanahan, S. F.; Hupp, J. T.; Danielson, E.; Meyer, T. J. *J. Phys. Chem.*, preceding article in this issue.

(2) (a) Hupp, J. T.; Otruba, J. P.; Parus, S. J.; Meyer, T. J. *J. Electroanal. Chem.* **1985**, *190*, 287. (b) Hupp, J. T.; Meyer, T. J. *J. Electroanal. Chem.*, in press. (c) Hupp, J. T.; Meyer, T. J., submitted for publication.

(3) Ellis, C. D.; Meyer, T. J. *Inorg. Chem.* **1984**, *23*, 1748.